Articles

Synthetic and Electrochemical Studies on 1,1′-Dithia-Substituted Derivatives of Ferrocene and Structure of 1,3-Dithia[3]ferrocenophane [$Fe(C_5H_4S)_2CH_2$]

Ralf Steudel,* Karin Hassenberg, and Joachim Pickardt

Institut für Chemie, Technische Universität Berlin, D-10623 Berlin, Germany

Emanuela Grigiotti and Piero Zanello*

Dipartimento di Chimica dell'Università di Siena, Via Aldo Moro, 53100 Siena, Italy

Received January 17, 2002

The bimetallic complexes fc(μ_2-S)$_2$TiCp$_2$ (**1**, fc = 1,1′-ferrocenyl, Cp = cyclopentadienyl) and fc(μ_2-S$_2$)(μ_2-S)TiCp$_2$ (**2**) were synthesized by reaction of fc(SH)$_2$ with Cp$_2$TiCl$_2$, and from fcS$_3$ and Cp$_2$Ti(CO)$_2$, respectively. The novel tetrasulfane fcS$_4$ was obtained from **2** and SCl$_2$. 1,3-Dithia[3]ferrocenophane fcS$_2$CH$_2$ was obtained from fc(SH)$_2$ and CH$_2$Cl$_2$ in the presence of Cp$_2$TiCl$_2$ and KOH. The molecular and crystal structure of fcS$_2$CH$_2$ was determined by X-ray crystallography; the molecular symmetry is C_s. Electrochemical studies on the recently prepared ferrocenophanes fcS$_2$-1-SO, fcS$_2$-1-SO$_2$, and fcS$_2$-2-SO show that, with respect to fcS$_3$, the progressive oxidation of the trisulfane bridge makes more and more difficult the fc/fc$^+$ oxidation, whereas insertion of a Cp$_2$Ti fragment exerts the opposite effect.

1,2,3-Trithia[3]ferrocenophane fcS$_3$ has been known for a long time from chemical,[1] structural,[2] and electrochemical studies.[3] Recently, the peroxo acid oxidation of fcS$_3$ afforded both the trisulfane-1-oxide fcS$_2$-1-SO and the corresponding sulfone fcS$_2$-1-SO$_2$, depending on the stoichiometry of the reactants.[4] The isomeric trisulfane-2-oxide fcS$_2$-2-SO was obtained from the dithiol fc(SH)$_2$ and thionyl chloride.[5] In an attempt to obtain access to more sulfur-rich derivatives fcS$_n$ with $n > 3$ we have synthesized the bimetallic ferrocenophanes fcS$_2$TiCp$_2$ (**1**) and fcS$_3$TiCp$_2$ (**2**) as potential precursors (Cp = η^5-C$_5$H$_5$) which should react with sulfur chlorides and organic sulfenyl chlorides to provide the corresponding novel ferrocene derivatives. In fact, the formerly unknown tetrasulfane fcS$_4$ was obtained from **2**. We also found a novel synthetic access to fcS$_2$CH$_2$, the molecular structure of which is reported for the first time. In addition, we report on the electronic effects caused by the replacement of the bridging S$_3$ chain for the sulfane oxide units S−S(=O)−S, S−S−S(=O), and S−S−S(=O)$_2$, respectively, as derived from electrochemical studies.

Syntheses. It was our aim to develop a synthetic access to the hitherto unknown 1,1′-ferrocene polysulfanes fcS$_n$ with $n > 3$. Since sulfur-rich organic polysulfanes are best prepared from suitable titanocene precursors by reaction with sulfur chlorides,[6] we tried the same route for the wanted ferrocene derivatives. The first step is the preparation of a suitable bimetallic double-sandwich complex like fc(μ_2-S)$_2$TiCp$_2$ (**1**) and fc(μ_2-S$_2$)-(μ_2-S)TiCp$_2$ (**2**) according to eqs 1 and 2, respectively.

Complexes **1** and **2** should then react with certain sulfur chlorides according to eq 3 to produce the corre-

* Corresponding authors. E-mail: steudel@schwefel.chem.tu-berlin.de and zanello@unisi.it.

(1) See, for example: (a) Brandt, P. F.; Rauchfuss, T. B. *J. Am. Chem. Soc.* **1992**, *114*, 1926. (b) Galloway, C. P.; Rauchfuss, T. B. *Angew. Chem.* **1993**, *105*, 1407; *Angew. Chem., Int. Ed. Engl.* **1993**, *32*, 1319. (c) Johnston, E. R.; Brandt, P. F. *Organometallics* **1998**, *17*, 1460. (d) Brandt, P. F.; Compton, D. L.; Rauchfuss, T. B. *Organometallics* **1998**, *17*, 2702.

(2) Davis, B. R.; Bernal, I. *J. Cryst. Mol. Struct.* **1972**, *2*, 107.

(3) (a) Sato, M.; Tanaka, S.; Ebine, S.; Morinaga, K.; Akabori, S. *J. Organomet. Chem.* **1985**, *282*, 247. (b) Beer, P. D.; Charlsley, S. M.; Jones, C. J.; McCleverty, J. A. *J. Organomet. Chem.* **1986**, *307*, C19. (c) Sidebotham, R. P.; Beer, P. D.; Hamor, T. A.; Jones, C. J.; McCleverty, J. A. *J. Organomet. Chem.* **1989**, *371*, C31. (d) Osborne, A. G.; Hollands, R. E.; Nagy, A. G. *J. Organomet. Chem.* **1989**, *373*, 229. (e) Ushijima, H.; Akiyama, T.; Kajitani, M.; Shimizu, K.; Aoyama, M.; Masuda, S.; Harada, Y.; Sugimori, A. *Bull. Chem. Soc. Jpn.* **1990**, *63*, 1015. (f) Zanello, P.; Opromolla, G.; Casarin, M.; Herberhold, M.; Leitner, P. *J. Organomet. Chem.* **1993**, *443*, 199. (g) Galloway, C. P.; Rauchfuss, T. B. *Angew. Chem.* **1993**, *105*, 1407; *Angew. Chem., Int. Ed. Engl.* **1993**, *32*, 1319. (h) Long, N. J.; Raithby, P. R.; Zanello, P. *J. Chem. Soc., Dalton Trans.* **1995**, 1245.

(4) Hassenberg, K.; Pickardt, J.; Steudel, R. *Organometallics* **2000**, *19*, 5244.

(5) Steudel, R.; Hassenberg, K.; Pickardt, J. *Organometallics* **1999**, *18*, 2910.

(6) Steudel, R.; Kustos, M. In *Encyclopedia of Inorganic Chemistry*; King, R. B., Ed.; Wiley: Chichester, 1994; Vol. 7, pp 4009−4038.

10.1021/om020041z CCC: $22.00
Publication on Web 05/24/2002

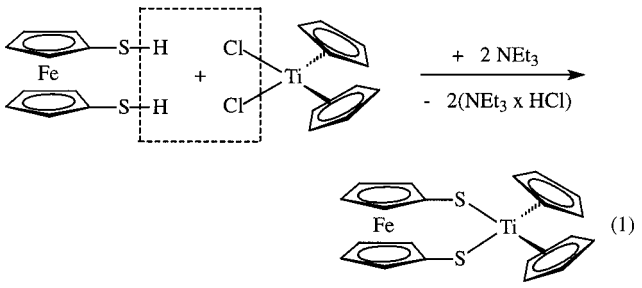

(1)

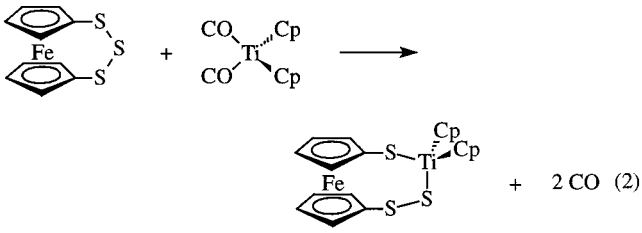

(2)

sponding ferrocene polysulfanes:

$$fcS_xTiCp_2 + S_nCl_2 \rightarrow fcS_{x+n} + Cp_2TiCl_2 \qquad (3)$$

The reaction according to eq 1 was carried out in toluene using the dithiol $fc(SH)_2$ prepared by reduction of fcS_3 with $LiAlH_4$.[7] Addition of NEt_3 to the red solution of $fc(SH)_2$ and Cp_2TiCl_2 resulted in a color change to dark green. After filtration the solvent was evaporated, leaving the crude product **1** as a black-green powder (yield 95%). This product produced a peak of relative intensity 35 for the molecular ion in the EI mass spectrum (base peak 100: Cp_2TiS^+). On reversed-phase HPLC analysis, one major and two much smaller peaks were observed. However, attempts to further purify the crude product on a preparative scale by conventional chromatographic separation resulted in decomposition. Nevertheless, the spectroscopic data support the formula, and the connectivity was established by reaction with $SOCl_2$, which produced the known trisulfane-2-oxide fcS_3O, as identified by IR, MS, and HPLC analysis and comparison to an authentic sample,[4] eq 4.

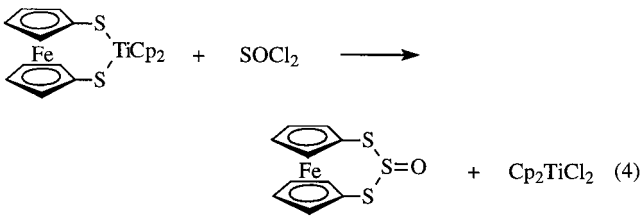

(4)

Because of the instability of **1**, we prepared complex **2** by the reaction shown in eq 2, which is in analogy with the many known insertion reactions of the titanocene unit into S−S bonds, using the dicarbonyl.[8] The brown solid of **2** (57% yield) was characterized by ^1H NMR, UV−vis, and MS spectroscopy. Reaction of **2** with 1 equiv of SCl_2 in carbon disulfide afforded 1,2,3,4-tetrathia[4]ferrocenophane fcS_4 in 27% yield (after chromatographic purification) as a yellow solid, eq 5.

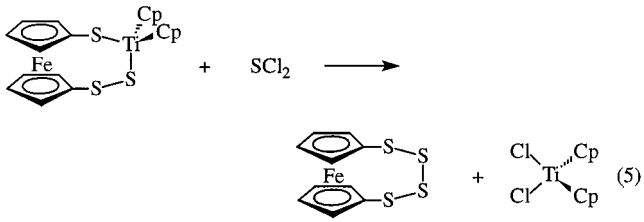

(5)

Both in solution and in the solid state fcS_4 slowly decomposes at room temperature to fcS_3 and S_8. The decomposition in the solid state can be slowed by cooling, but even at −55 °C some decomposition occurred.

When we tried to synthesize **1** from $fc(SH)_2$ and Cp_2TiCl_2 in dichloromethane in the presence of KOH, we surprisingly obtained fcS_2CH_2 instead (yield 35%), eq 6.

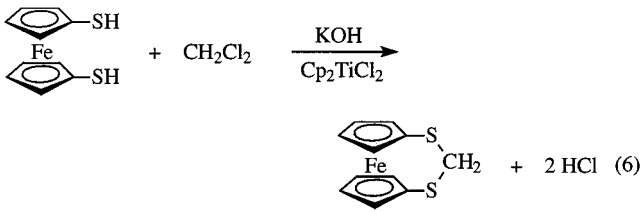

(6)

For this reaction to occur, the presence of Cp_2TiCl_2 is not mandatory but the reaction is much slower without Cp_2TiCl_2, which evidently functions as a catalyst. 1,3-Dithia[3]ferrocenophane fcS_2CH_2 had previously been synthesized from $fc(SH)_2$ and CH_2I_2[9] and characterized spectroscopically. The product was described as orange crystals[9,10] Our crude product from reaction 6, precipitated at −55 °C, was dark green, obviously owing to some admixed fcS_2TiCp_2 **1**, which is a likely byproduct. Recrystallization of the crude product from CS_2 produced yellow crystals. When the synthesis was carried out in the absence of Cp_2TiCl_2, the yield was much lower and the crude product was orange-yellow. The melting temperature (182 °C) agrees with the literature values, as does the ^1H NMR spectrum.[9,10] Even at the melting temperature no decomposition was observed. Since the crystal structure of fcS_2CH_2 had remained unknown, we performed an X-ray diffraction analysis on single crystals.

X-ray Structural Analysis of fcS_2CH_2. Orthorhombic crystals of fcS_2CH_2 were obtained by partial evaporation of a solution in CS_2 at 4 °C. The molecular structure is depicted in Figure 1. The molecular symmetry is C_s. The two cyclopentadienyl rings are eclipsed and almost parallel (interplanar angle 4.59°, closing toward the bridge). The molecular parameters all seem to have normal values.

Electrochemistry. Figure 2 compares the cyclic voltammetric response given by the precursor fcS_3 with those of trisulfane-1-oxide, $fc[3]S_2$-1-SO, and trisulfane-1,1-dioxide, $fc[3]S_2$-1-SO_2, in dichloromethane solution.

(7) Bishop, J. J.; Davison, A.; Katcher, M. L.; Lichtenberg, D. W.; Merrill, R. E.; Smart, J. C. *J. Organomet. Chem.* **1971**, *27*, 241.

(8) See, for example: (a) Bergemann, K.; Kustos, M.; Krüger, P.; Steudel, R. *Angew. Chem.* **1995**, *107*, 1481; *Angew. Chem., Int. Ed. Engl.* **1995**, *34*, 1330. (b) Steudel, R.; Kustos, M.; Münchow, V.; Westphal, U. *Chem. Ber./Recl.* **1997**, *130*, 757. (c) Steudel, R.; Schumann, O.; Buschmann, J.; Luger, P. *Angew. Chem.* **1998**, *110*, 515; *Angew. Chem., Int. Ed.* **1998**, *37*, 492.

(9) Davison, A.; Smart, J. C. *J. Organomet. Chem.* **1979**, *174*, 321.

(10) Abel, E. W.; Booth, M.; Brown, C. A.; Orrell, K. G.; Woodford, R. L. *J. Organomet. Chem.* **1981**, *214*, 93.

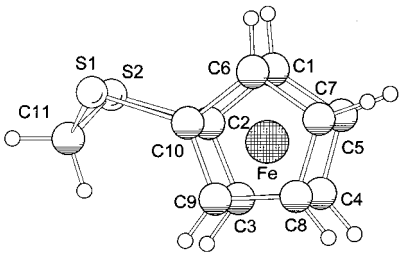

Figure 1. Molecular structure of fcS_2CH_2 in the crystal. Selected internuclear distances (Å) and angles (deg): S(1)−C(11) = 1.817(3), S(2)−C(11) = 1.812(2), S(1)−C(10) = 1.755(2), S(2)−C(2) = 1.756(2), C(11)−H(1a) = 0.970, C(10)−S(1)−C(11) = 101.7(1), S(1)−C(11)−S(2) = 115.8-(1), C(11)−S(2)−C(2) = 102.25, S(1)−C(11)−H(11a) = 108.3, C(10)−S(1)−C(11)−S(2) = −74.8(1).

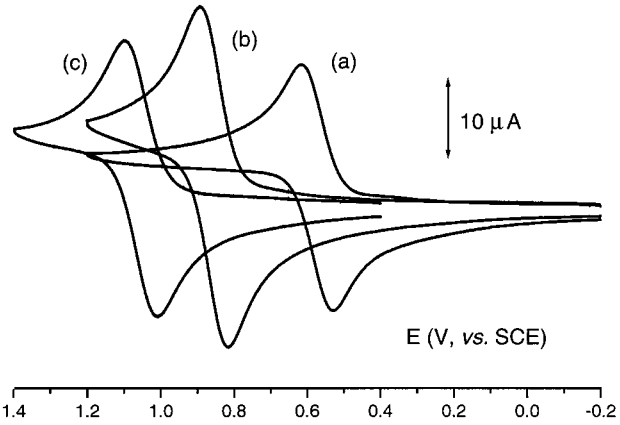

Figure 2. Cyclic voltammograms recorded at a platinum electrode on CH_2Cl_2 solutions containing $[NBu_4][PF_6]$ (0.2 mol dm^{-3}) and (a) fcS_3 (1.1×10^{-3} mol dm^{-3}); (b) fcS_2-1-SO (1.3×10^{-3} mol dm^{-3}); and (c) fcS_2-1-SO_2 (1.2×10^{-3} mol dm^{-3}). Scan rate 0.2 V s^{-1}.

As expected, all investigated complexes exhibit the reversible ferrocene/ferrocenium oxidation. In fact, controlled potential coulometry in correspondence to the respective anodic processes consume one electron per molecule. In each case the resulting solutions exhibit voltammetric profiles quite complementary to the original ones, thus testifying to the chemical reversibility of the respective one-electron removals.

Analysis of the cyclic voltammetric responses with a scan rate varying from 0.02 to 1.00 V s^{-1} shows that the current ratio i_{pc}/i_{pa} is constantly equal to 1 (in agreement with controlled potential coulometric results), the current function $i_{pa}v^{-1/2}$ stays constant, and the peak-to-peak separation ΔE_p is around 70−80 mV at low scan rates (from 0.02 to 0.1 V s^{-1}) and slightly increases to 90−100 mV at higher scan rates. Taking into account that under the same experimental conditions unsubstituted ferrocene displays a similar voltammetric trend, we assume that the oxidation process of the present ferrocenophanes is substantially reversible from the electrochemical viewpoint, which implies that no significant geometrical reorganization would follow the electron removal processes.

In Table 1 the formal electrode potentials of the mentioned processes are compiled. These data confirm the previous finding that in the sequence $fc[3](CH_2)_3$/$fc[3]S_2$-2-CH_2/$fc[3]S_3$ the progressive substitution of methylene groups for sulfur atoms makes the oxidation process more and more difficult.[3e] It is however also evident that a similar inductive effect takes place upon progressive oxygenation of the bridging sulfur atoms according to the sequence $fc[3]S_3$/$fc[3]S_2$-1-SO (or, $fc[3]S_2$-2-SO)/$fc[3]S_2$-1-SO_2. Such a remarkable electron-withdrawing effect played by the oxygen atoms on the other hand agrees well with the results obtained upon substitution of one methylene group for a carbonyl group in 1,2,3-trimethylene[3]ferrocenophane.[11]

Table 1. Formal Electrode Potentials (V, vs SCE), Peak-to-Peak Separations (mV), and Maximum Wavelength (nm) for the Ferrocene-Centered Redox Processes Exhibited by the Present Ferrocenophanes

complex	$E^{o\prime}_{(0/+)}$	ΔE_p[a]	E_p[a,b]	λ_{max}[c]	solvent	reference
fcS_3	+0.67	85		375	CH_2Cl_2	3h
	+0.69				MeCN	3e
fcS_2-1-SO	+0.86	72	−1.31	630	CH_2Cl_2	this work
fcS_2-2-SO	+0.82	78	−1.42	665	CH_2Cl_2	this work
fcS_2-1-SO_2	+1.05	72	−1.46	620	CH_2Cl_2	this work
fcS_2-2-CH_2	+0.66	100		690	CH_2Cl_2	this work
	+0.60				MeCN	3e
$fc(CH_2)_2$-2-S	+0.41				MeCN	3e
$fc(CH_2)_3$	+0.33				MeCN	11
$fc(CH_2)_2$-1-CO	+0.62				MeCN	11
fcS_3TiCp_2	+0.20	78	−1.31[d]		CH_2Cl_2	this work
fcH	+0.39	78		620	CH_2Cl_2	this work
	+0.38	64		620	MeCN	this work

[a] Measured at 0.2 V s^{-1}. [b] Peak-potential value for irreversible processes. [c] Absorbance of the electrogenerated ferrocenium congeners. [d] Formal electrode potential measured at 2.0 V s^{-1}.

It is also interesting to note that in the series $fc[3](CH_2)_{3-n}S_n$ a linear trend exists as far as the oxidation potentials and number of sulfur atoms are concerned (correlation coefficient 0.99). Under the assumption that the same additive electronic effects hold in the series $fc[4](CH_2)_{4-n}S_n$, from the known oxidation potentials of the two members $fc[4](CH_2)_4$ (+0.30 V, in MeCN)[11,12] and $fc[4](CH_2)_2(1,4\text{-}S)_2$ (+0.61 V, in MeCN)[3a] an oxidation potential of 0.92 V (in MeCN) can be predicted for the labile $fc[4]S_4$.

It deserves attention that exhaustive one-electron oxidation of fcS_3 does not induce color changes with respect to the original yellow solution, whereas the electrogenerated monocations $[fc[3]S_2\text{-}1\text{-}SO]^+$, $[fc[3]S_2\text{-}2\text{-}SO]^+$, and $[fc[3]S_2\text{-}1\text{-}SO_2]^+$ assume a pale green color. Taking into account that iron-centered ferrocenium species are green to blue colored ($\lambda_{max} \approx 620$ nm), it can be speculated that while the trisulfur bridge highly contributes to the HOMO level of fcS_3, thus to prevail over the iron contribution, oxygen functionalization seems to restore the iron-centered character of the HOMO levels. In fact, the oxygenated monocations display a flat band in the region from 620 to 670 nm, assignable to their partial iron-centered character.

Finally, Figure 3 shows the cyclic voltammetric behavior of fcS_3-2-$TiCp_2$.

As can be seen from the voltammetric profile in Figure 3a, the presence of the $TiCp_2$ fragment in the bridge significantly affects the redox pattern with respect to those discussed above. Let us first discuss the anodic part. A first anodic process, with features of chemical

(11) Toma, Š.; Solčániová, E.; Nagy, A. G. *J. Organomet. Chem.* **1985**, *288*, 331.
(12) Fujita, E.; Gordon, B.; Hilmann, M.; Nagy, A. G. *J. Organomet. Chem.* **1981**, *218*, 105.

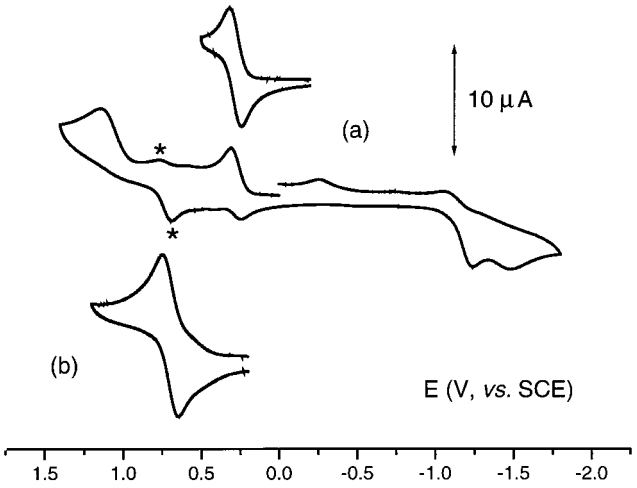

Figure 3. Cyclic voltammograms recorded at a platinum electrode on a CH_2Cl_2 solution of fcS_3-2-$TiCp_2$ (1.3×10^{-3} mol dm^{-3}). $[NBu_4][PF_6]$ (0.2 mol dm^{-3}) supporting electrolyte. (a,b) Original response; (b) after exhaustive oxidation at the first anodic step. Scan rate 0.2 V s^{-1}.

reversibility, is followed by a second irreversible oxidation ($E_p = +1.08$ V). In addition, a minor peaks system (starred) appears after traversing the first, ferrocene-centered oxidation. Such a profile predicts that the starred peaks system may be due to a new species arising from slow chemical complications following the ferrocene-centered oxidation (in fact, the current ratio i_{pc}/i_{pa} of the first anodic process is equal to 0.7 at 0.02 V s^{-1} and then tends to increase with the scan rate, reaching the unity value at 1.0 V s^{-1}). As a matter of fact, exhaustive oxidation in correspondence to the first anodic process ($E_w = +0.5$ V) makes the brown color of the original solution turn yellow, affording concomitantly a new species, which gives rise to a reversible peaks system ($E^{\circ\prime} = +0.7$ V) just coincident with the above-mentioned starred peaks system in Figure 3b. We did not succeed in identifying such a new product by mass spectrometry. In view of the highest oxidation state of Ti in the $TiCp_2$ fragment, the irreversible oxidation at high potential values is attributed to a sulfur-centered electron removal.

As far as the cathodic path is concerned, in agreement with previous assignments on ferrocene-titanium derivatives,[13] the partially chemically reversible reduction is easily assigned to the Ti(IV)/Ti(III) reduction of the bridging Ti(IV) fragment. In this case the electron addition is also complicated by fast degradation reactions. In fact, the relative current ratio, i_{pa}/i_{pc}, is 0.2 at 0.2 V s^{-1} and tends to increase with the scan rate, reaching the value of 0.4 at 2.0 V s^{-1}. It is interesting to note the strong electron-donating effect played by the $TiCp_2$ fragment, which makes the oxidation of fcS_3-2-$TiCp_2$ easier by about 0.4 V with respect to fcS_3.

In summary, we have evaluated by electrochemical investigations the electronic effects played by the oxygen atoms of different sulfane oxides in tri- and dithiaferrocenophanes. We have also shown that heterobimetallic complexes of ferrocene with titanocene can be prepared,[14] which should be useful precursors for the preparation of many novel ferrocene derivatives by reaction with suitable sulfur-chlorine compounds, as has been shown for other titanocene dithiolato complexes.[6,15]

Experimental Section

General Considerations. All syntheses were performed under an atmosphere of nitrogen. Solvents were dried and distilled prior to use. ^1H and ^{13}C NMR spectra were recorded at room temperature on Bruker ARX200 and ARX400 instruments. Mass spectra were measured with an AMS Intectra instrument, based on Varian MAT 311A equipment. UV−vis spectra were obtained with a Waters 990 diode-array detector (190−800 nm) connected on-line to the HPLC equipment. Elemental analyses were performed on a Perkin-Elmer 2700 CHNS analyzer. Materials and apparatus for electrochemistry have been described elsewhere.[16] All potential values refer to the saturated calomel electrode (SCE).

Preparation of [fc(μ_2-S)$_2$TiCp$_2$] (1). To a solution of Cp_2TiCl_2 (309 mg, 1.24 mmol) in 80 mL of toluene are added 331 mg of $fc(SH)_2$ (1.24 mmol) and 250 mg of Et_3N (2.48 mmol). After stirring for 4 h at room temperature the dark green solution is filtered and the solvent evaporated in a vacuum, resulting in a black-green residue of crude **1** (497 mg). ^1H NMR (C_6D_6): δ 3.94 (dt, 2H), 4.08 (m, 2H), 4.14 (dt, 2H), 4.25 (m, 2H), 5.80 (s, 10H). UV−vis (methanol): 215, 240, 303, 432, 640 nm. MS (249 °C, *m*/*z*): 426 (35, M^+), 361 (40, $M - Cp^+$), 248 (30, fcS_2^+), 209 (100, $Cp_2TiS - H^+$), 186 (44, Cp_2Fe^+), 178 (31, Cp_2Ti^+).

Preparation of [fc(μ_2-S)(μ_2-S$_2$)TiCp$_2$] (2). To a solution of fcS_3 (239 mg, 0.854 mmol) in 80 mL of *n*-hexane is added dropwise within 1 h a solution of $Cp_2Ti(CO)_2$ (200 mg, 0.854 mmol) in 50 mL of *n*-hexane. The brown precipitate of **2** is isolated and washed twice with *n*-hexane (223 mg, 57%). ^1H NMR ($CDCl_3$): δ 3.83 (m, 2H), 4.36 (m, 2H), 4.44 (m, 2H), 4.52 (m, 2H), 6.59 (s, 10H). $^{13}C\{^1H\}$ NMR ($CDCl_3$): δ 67.92, 69.07, 69.82, 70.60, 76.10, 111.58, 113.66. UV−vis (methanol): 224, 293, 333, 405, 765 nm. Anal. Calcd for $C_{20}H_{18}FeTiS_3$: C, 52.41; H, 3.95; S, 20.99. Found: C, 51.81; H, 4.20; S, 20.58.

Preparation of [fcS$_4$]. To a solution of **2** (230 mg, 0.50 mmol) in 30 mL of CS_2 is added a solution of SCl_2 (52 mg, 0.50 mmol) in 1.6 mL of CS_2. After the color has changed from brown to orange-red the precipitated Cp_2TiCl_2 is filtered off and the solution stirred with a little silica gel to bind residual Cp_2TiCl_2 (color change to yellow). After filtration the solvent is evaporated and the residue purified by column chromatography on silica gel (mobile phase: dichloromethane/*n*-hexane, 1:4 v/v), yielding 42 mg of fcS_4 (27%). ^1H NMR ($CDCl_3$): δ 4.41 (pt, 4H), 4.75 (pt, 4H). UV−vis (methanol): 220, 293, 392, 450 nm. Anal. Calcd for $C_{10}H_8FeS_4$: C, 38.46; H, 2.58; S, 41.07. Found: C, 37.83; H, 2.60; S, 40.52.

Preparation of [fc(μ_2-S)$_2$CH$_2$]. To a solution of $fc(SH)_2$ (113 mg, 0.45 mmol) in 15 mL of dichloromethane are added 102 mg of solid Cp_2TiCl_2 (0.41 mmol) and 4.1 mL of aqueous KOH (5%), resulting in a color change of the organic phase from red to almost black while the aqueous phase becomes red. After stirring at room temperature for 2 h the phases are separated and the organic layer is dried over $MgSO_4$. After filtration and partial evaporation of the solvent the product is precipitated by adding *n*-hexane and cooling to −55 °C, resulting in a dark green solid of mp 182 °C (38 mg, 35%). ^1H NMR ($CDCl_3$): δ 4.12 (s br, 4H), 4.17 (s, 2H), 4.35 (m, 4H). UV−vis (methanol): 214, 268, 414 nm. Anal. Calcd for $C_{11}H_{10}FeS_2$: C, 50.39; H, 3.84; S, 24.45. Found: C, 49.97; H, 3.51; S, 23.82.

(13) (a) Hayashi, Y.; Osawa, M.; Wakatsuki, Y. *J. Organomet. Chem.* **1997**, *542*, 241. (b) Back, S.; Pritzkow, H.; Lang, H. *Organometallics* **1998**, *17*, 41.

(14) For other ferrocene-titanium complexes, see for example: (a) Gibson, V. C.; Long, N. J.; Martin, J.; Soslan, G. A.; Stichbury, J. C. *J. Organomet. Chem.* **1999**, *590*, 115. (b) Shafir, A.; Arnold, J. *J. Am. Chem. Soc.* **2001**, *123*, 9212.

(15) Steudel, R. *Chem. Rev.*, in press.

(16) Togni, A.; Hobi, M.; Rihs, G.; Albinati, A.; Zanello, P.; Zech, D.; Keller, H. *Organometallics* **1994**, *13*, 1224.

Table 2. Crystal Data, Data Collection, and Structure Refinement for fcS_2CH_2

formula	$C_{11}H_{10}FeS_2$
fw	262.16
color	yellow
cryst size, mm	0.82 × 0.64 × 0.46
cryst syst	orthorhombic
space group	*Pcab*
temp, K	293(2)
wavelength, Å	0.71073
a, Å	9.61490(10)
b, Å	11.8570(2)
C, Å	17.87610(10)
V, Å^3	2037.94(4)
Z	8
density (calcd), g cm^{-3}	1.709
abs coeff, mm^{-1}	1.8400
F(000)	1072
scan range, deg	$2.28 \leq 2 \leq 30.47$
no. of reflns collected	17 434
no. of ind reflns	3081 ($R_{int} = 0.0689$)
refinement method	full matrix, least squares on F^2
no. of data/restraints/params	3081/0/160
goodness-of-fit on F^2	0.939
final *R* indices [$I > 2\sigma(I)$]	R1 = 0.0328, wR2 = 0.0898
R indices, all data	R1 = 0.0424, wR2 = 0.0989
largest diff peak and hole, e Å^{-3}	0.348, −0.308

X-ray Diffraction Study. The details of the crystal structure determination and refinement are given in Table 2. Data were collected on a Siemens Smart CCD diffractometer using Mo Kα radiation ($\lambda = 0.71069$ Å). The structure was solved after *Lp* and absorption correction (SADABS[17]) by direct methods (SHELXS[18]) and refined with anisotropic thermal parameters for the non-hydrogen atoms (SHELXL[19]). Hydrogen positions at the ring atoms were refined with a riding model. The drawing was created with the DIAMOND program.[20]

Crystallographic data have been deposited at the Cambridge Data Center and may be obtained free of charge on quoting the depository number CCDC 175495 from CCDC, 12 Union Road, Cambridge CB2 1EZ, UK (fax: +44-1223-336033, e-mail: deposit@ccdc.cam.ac.uk).

Acknowledgment. This work was supported by the Deutsche Forschungsgemeinschaft and the Verband der Chemischen Industrie. P.Z. gratefully acknowledges the financial support from the University of Siena (PAR 2001).

Supporting Information Available: Tables with bond lengths, bond angles, torsion angles and atomic coordinates have been deposited. This material is available free of charge via the Internet at http://pubs.acs.org.

OM020041Z

(17) Sheldrick, G. M. *SADABS*, Empirical Absorption Correction Program; Göttingen, 1996.
(18) Sheldrick, G. M. *SHELXS-97*, Program for Crystal Structure Solution; Göttingen, 1997.
(19) Sheldrick, G. M. *SHELXL-97*, Program for Refinement of Crystal Structures; Göttingen, 1997.
(20) Bergerhoff, G.; Brandenburg, K.; Berndt, M. *DIAMOND*, Visuelles Informationssystem für Kristallstrukturen; Bonn, 1996.